

Article

Blood cell count using Deep Learning Semantic Segmentation

Thanh Tran Thi Phuong¹, Lam Binh Minh², Suk-Hwan Lee³ and Ki-Ryong Kwon^{1,*}

¹ Dept. of IT Convergence and Applications Engineering, Pukyong National University, Busan, South Korea; thanhttp02@gmail.com

² Dept. of Electronic Engineering, Pukyong National University, Busan, South Korea; lbminh2015@gmail.com

³ Dept. of Information Security, Tongmyong University, Busan, South Korea; skylee@tu.ac.kr

* Correspondence: krkwon@pknu.ac.kr; Tel.: +82-051-629-6257

Abstract: Clinically, knowing the number of red blood cells (RBCs) and white blood cells (WBCs) helps doctors to make the better decision on accurate diagnosis of numerous diseases. The manual cell counting is a very time-consuming and expensive process, and it depends on the experience of specialists. Therefore, a completely automatic method supporting cell counting is a viable solution for clinical laboratories. This paper proposes a novel blood cell counting procedure to address this challenge. The proposed method adopts SegNet - a deep learning semantic segmentation to simultaneously segment RBCs and WBCs. The global accuracy of the segmentation of WBCs, RBCs, and the background of peripheral blood smear images obtains 89% when segment WBCs and RBCs from the background of blood smear images. Moreover, an effective solution to separate grouped or overlapping cells and cell count is presented using Euclidean distance transform, local maxima, and connected component labeling. The counting result of the proposed procedure achieves an accuracy of 93.3% for red blood cell count using dataset 1 and 97.38% for white blood cell count using dataset 2.

Keywords: Complete blood count; deep learning; segmentation; SegNet; Vgg-16.

1. Introduction

The complete blood count (CBC) is typically performed to determine the number of white blood cells (WBCs), red blood cells (RBCs), and platelet (PLTs) in a person's sample blood [1]. Medically, CBC can help doctors evaluate the overall health of a patient. The number of any components in a blood smear that are too high or too low could signal the medical problem. For instance, a low number of white blood cells count called Leukopenia can be triggered by HIV, bone marrow disorders, lymphoma, severe infections, liver and spleen diseases. A high RBC count called erythrocytosis may be caused by congenital heart disease, dehydration, renal cell carcinoma, pulmonary fibrosis, polycythemia vera. If the patient has the abnormal results in the CBC test, doctors may require the patient to perform other tests to find out the cause of abnormal blood cell counts.

To estimate the number of cells, a laboratory technician examines a blood sample under a microscope. However, the manual blood cell counts are extreme fatigue for the trained laboratorian. Furthermore, the results of counting are not reliable due to a large number of blood cells in the peripheral smear. Consequently, an automated or semi-automated procedure to support blood cell count on blood smear images is very helpful for clinical purpose.

The proposed method presents two separate phases of segmentation and blood cell count. The main target of the segmentation phase is to segment WBCs and RBCs by adopting SegNet architecture. Most previous works mainly focused on the segmentation of leucocytes in images using various segmentation techniques. Research in [2] combined watershed segmentation with a shift-invariant complex transform for the segmentation of WBCs. Wei Gao et. al. In [3], N. H. Harun et. al.

experimented three clustering algorithms including k-means, fuzzy c-mean, and moving k-means clustering for abnormal WBCs segmentation.

For the blood cell counting phase, according to literature, few works of blood cell counting system that are count simultaneous the number of WBCs and RBCs. Research in [4] utilized various conventional image processing methods to enhance the quality of images. In the next steps, J. Poomcokrak and C. Neatpisarnvanit classified only red blood cells and counted the number of red blood cells by a neural network. The accuracy for counting red blood cells was not too high, reached 74%. The restriction of this paper only focuses on red blood cells counting. WBC count was not included in this paper. In another study, Navin D. Jambhekar [5] demonstrated image processing techniques to classify only red blood cells. First, edge detection, feature extraction, and histogram were utilized to detect red blood cells. And the next second a shallow neural network with three layers was used for counting red blood cells. The accuracy of this paper reached 81%. In [6], Joost Vromen and Brendan McCane calculated a gradient magnitude map and traced the contours of overlapping cells using Bayesian method associated with a polynomial model to smooth boundaries of cells. The supervised methods achieved an accuracy of 82.5% for red blood cells count. The methods in [7] focused on counting red blood cells using a circular Hough transform. Beforehand, conventional image processing techniques are utilized to separate cells from the background. The accuracy of this paper for counting red blood cells achieved 91.87% when conducting on small dataset including 10 images. The drawback of the aforementioned works are conducted on the small dataset with the accuracy is not too high.

Lorenzo Putzu and Cecilia Di Ruberto alternated between using image processing techniques and segmentation to detect white blood cells in microscopic images [8], [9]. Firstly, they identified the background of images using Zack algorithm. Then, histogram equalization was applied on component from CMYK color model of the image for WBCs identification. L. Putzu et. al. used watershed segmentation to separate the grouped of WBCs. They reported that the accuracy of their method for WBC count reached 92% when performed on 33 testing images. K. Jha et. al. [10] proposed using a set of image processing techniques and morphological methods for segmenting blood cells and counting the number of WBCs. The method was evaluated on twenty images and obtain an accuracy of 85% for WBC count. Research in [11] also detected white blood cells by image processing techniques such as Zack algorithm, histogram. Z. Alreza and A. Karimian separated clumped leucocytes by using the watershed segmentation method. Then, they extracted features, including texture, color, average, variance, standard deviation, and entropy features. These features were utilized for SVM classification model. Their methods reached the accuracy of 93% for leucocytes counts.

These above methods of segmentation and blood cell count still do remained some drawbacks. For example, there is only few works addressed the challenge to separate high overlapping cells and count blood cells. Besides, most blood cells in peripheral blood images exist in different shape, color, and characteristic. For example, white blood cells (leucocytes) are divided into five types with different shapes and color based on their function: monocytes, lymphocytes, eosinophils, neutrophils, and basophils, as shown in Figure 1. Moreover, the quality of peripheral blood cell images is also affected by acquisition condition, such as illuminance. Hence, an effective methodology to segment and count blood cells with compromising accuracy is necessary. In this research, we proposed a system included the segmentation phase and the counting phase. SegNet architecture is utilized in the segmentation phase for the semantic segmentation of WBCs, RBCs, and the background of images. The segmented result images of this phase are employed as the input for the counting phase. Distance transform and connected component labelling are utilized to handle with touching cells.

The rest of this paper is organized as follows. Section 2 introduces about materials and methods. The experiment result and discussion are shown in section 3. Finally, the conclusion is illustrated in section 4.

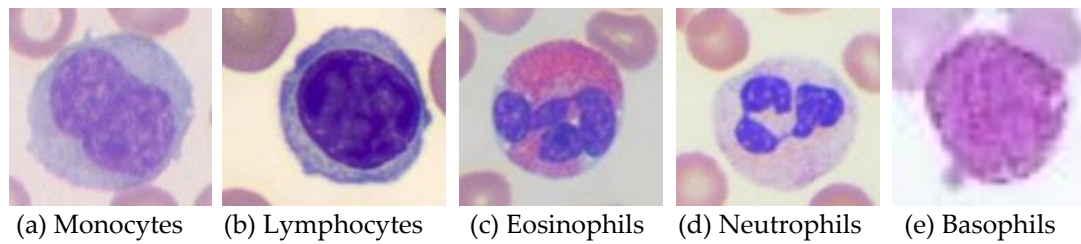


Figure 1. The shape of the five major types of white blood cells.

2. Materials and Methods

2.1. Dataset Processing

In this research, the ALL-IDB1 dataset is used for the experiment. The corresponding segmentation ground truth images are necessary for the semantic segmentation. Hence, GNU Image Manipulation Program (GIMP 2.10.2) is conducted to manually label peripheral blood smear images for the blood cell segmentation. It takes a long time to create the ground truth (mask) for the original images due to a large number of red blood cells in smear images. Hence, to evaluate our proposed method on white blood cell segmentation and counts, we crop a part of each image in ALL-IDB1. This cropped images and the corresponding ground truth images are called dataset 1. An example of a blood smear image and its mask is depicted in Figure 2. Dataset 1 is a collection of images containing 42 images and 42 ground truth images. The ground truth images in this dataset provide pixel-level labels for three classes including red blood cells, white blood cells, and the background. In figure 2, the blue color indicates red blood cells, the green color indicates white blood cells, and the yellow color indicates the background.

In dataset 2, 101 images in ALL-IDB1 are annotated as ground truth. Dataset 2 is used to evaluate the performance of WBC count. Therefore, rather than dwelling on the classification of RBCs, WBCs, and background, images in dataset 2 are annotated as two classes. All of WBCs in images are annotated as the green color, the other cells and background of images are considered as the background and annotated as the yellow color, as illustrated in Figure 3.

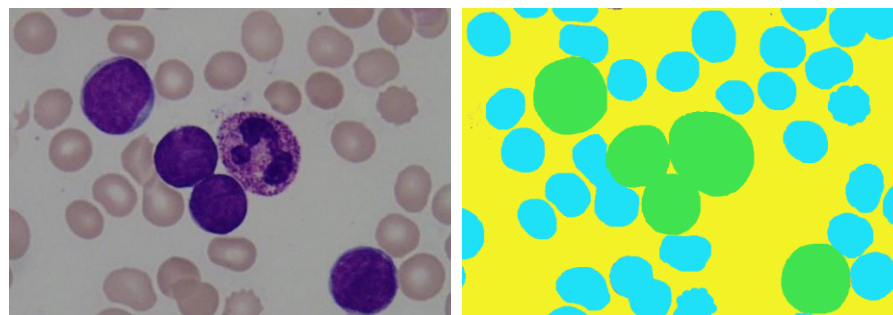


Figure 2. A peripheral blood smear image and its ground truth in dataset 1.

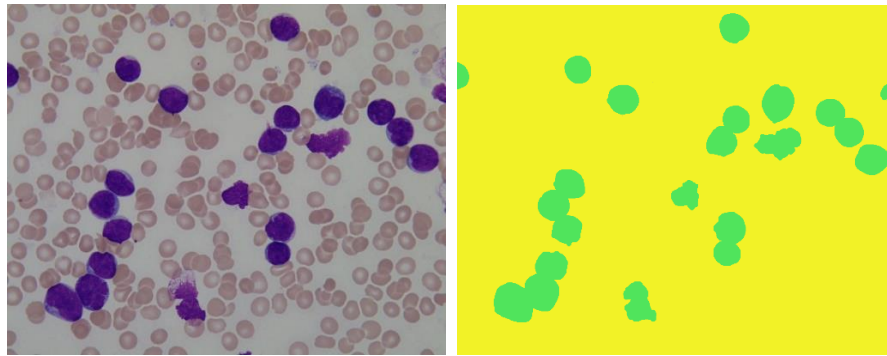


Figure 3. A peripheral blood smear image and its ground truth in dataset 2.

2.2. System overview

The proposed framework is shown in Figure 4. It includes two phases, segmentation and counting clumped cells. Segmentation phase performs SegNet to output semantic segmented images, in which RBCs are marked as blue, WBCs are marked as green, and the background is marked as yellow. Clumped cell counting phase is in charge of segmenting touching cells and counting cells in images. Section 2.2.1 and 2.2.2 present the detailed description of the two phases.

2.2.1. Segmentation

In computer vision, object detection is more popular for locating and classifying objects in the image. Since object detection algorithms, such as R-CNN and Yolo detect objects by drawing bounding rectangles around them, these detected objects do not obtain exactly the shape of objects. Semantic segmentation overcomes these aforementioned weakness because it classifies each and every pixel in the image. Therefore, semantic segmentation can detect accurately the boundary or edge of objects in the image, instead of drawing only boxes around objects.

In this work, we apply SegNet architecture to efficiently segment WBCs and RBCs in the image. SegNet is a deep architecture for the segmentation of multi-class based on assigning each pixel of an image into a corresponding class [12]. The SegNet architecture consists of Encoder and Decoder network, as shown in Figure 5. Encoder architecture composes three types of layers: convolution, batch normalization, and pooling layers. Because the max-pooling layer in Encoder reduces the size of the feature map, the boundary of cells in the image can be blurred. Therefore, the boundary information is stored in encoder feature maps. The decoder uses max-pooling indices stored in each encoder map to upsample the feature map.

In this paper, SegNet model is developed using weights initialized by the VGG-16. The additional layers required for segmentation replace the last pooling layer for classification from the pre-trained VGG-16. A label image produced via SegNet network is comprised of labeled pixels with corresponding colors. Of these, RBCs which are in blue color, WBCs are in green, and the background is in yellow, as can be seen from Figure 4. Then, all RBCs and WBCs are separated into two individual images with corresponding colors. The resulted images are used as the input of the counting phase to count the number of RBCs and WBCs expounded on section 2.2.2. Furthermore, they can be used as the input of a convolutional neural network to early detect leukemia – a type of white blood cell cancer.

2.2.2. Blood cell count

RBCs and WBCs images are used as the input image for the clumped cell counting phase, as illustrated in Figure 4. Cells in an image are touched or overlapped with other cells. First, images are converted to binary images. In the next step, distance transform (DT) is applied to these image for analyzing the skeleton of blood cells. We utilize distance transform using four distance metrics includes Euclidean DT, Chessboard DT, City block DT, and Quasi-Euclidean DT. The experiment results figure out that Euclidean DT shows the best approximate results for our purpose. For each

pixel in a binary image, Euclidean DT assigns a value which is the distance from the current pixel to the nearest non-zero pixel. The formula for Euclidean DT is defined as:

$$D_{Euclidean} = \sqrt{(x_2 - x_1)^2 + (y_2 - y_1)^2} \quad (1)$$

Where two pixels have coordinates (x_1, y_1) , (x_2, y_2) .

Figure 6 shows an example binary image, and the distance transform of a WBCs image.

In the next step, binary dilation is used for enlarging the cell shapes contained in distance transform images. Each pixel in a distance transform image is superimposed with the center of a 3-by-3 array of ones. The local maxima is propagated, as shown in Figure 7 (a). Small size cells, i.e., cells with the size of less than 30% or incomplete blood cells are discarded. Each cell will be labelled with different colors, as shown in Figure 7 (b). Finally, connected component labeling algorithm is performed to count the number of separated cells in images.

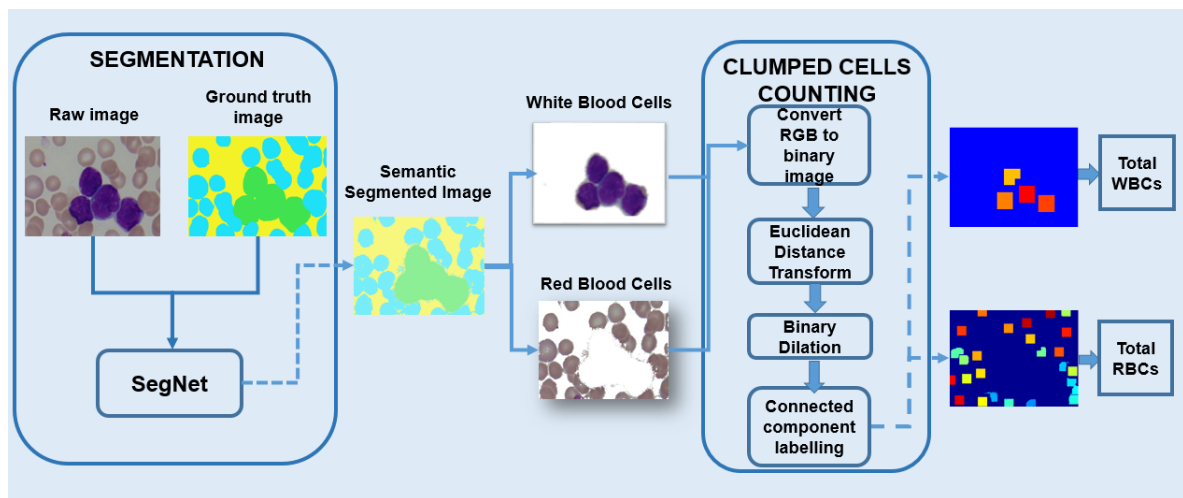


Figure 4. Our proposed procedure.

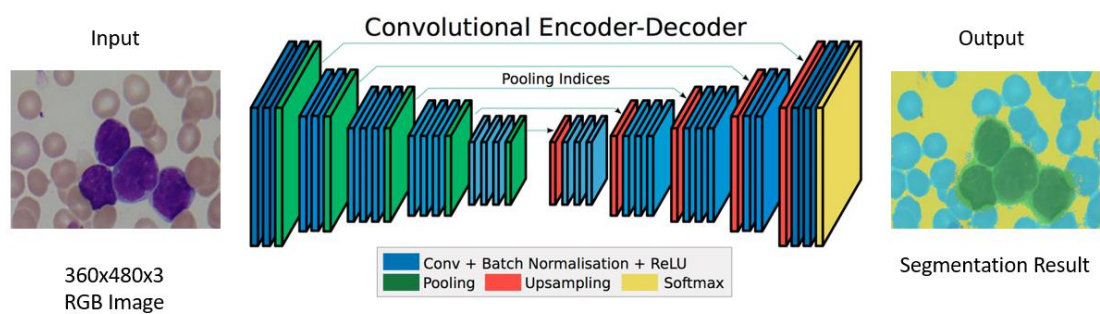


Figure 5. SegNet architecture [12].

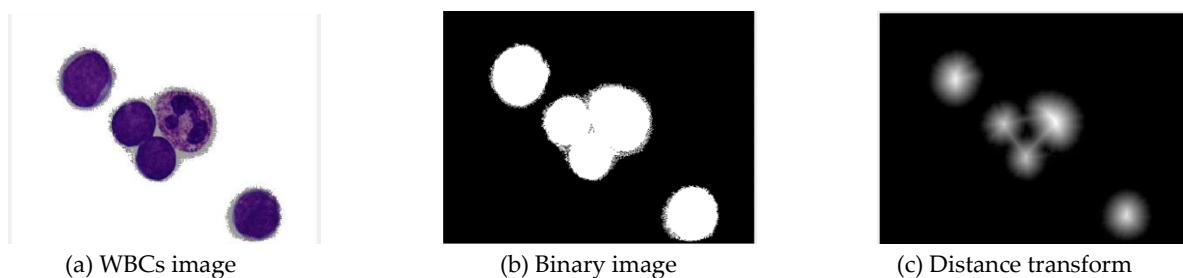


Figure 6. An example of distance transform.

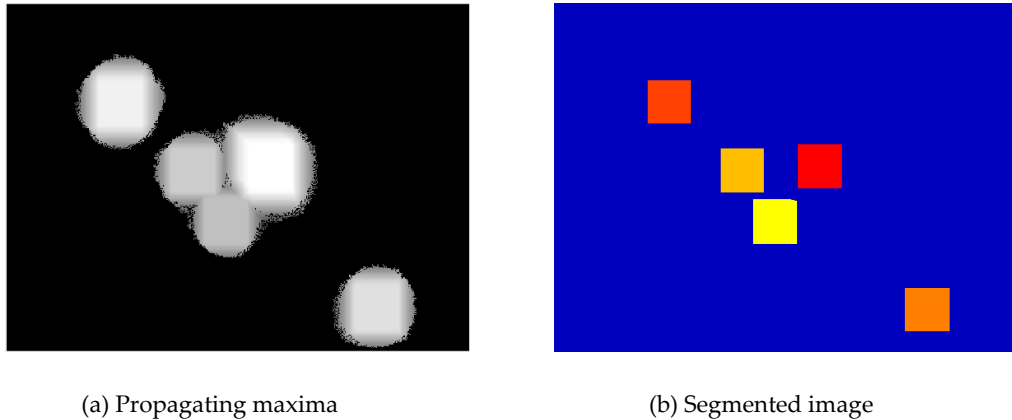


Figure 7. Propagating maxima and segmented of clumped cells in the image.

3. Experiment results and discussion

3.1. Metrics to evaluate the performance of SegNet

3.1.1. Accuracy

Global accuracy gives an overview of the portion of the correctly classified pixels to the total number of pixels in the image. Global accuracy is a metric calculated by dividing the correctly classified pixels (the sum of true positive TP and true negative TN) by the total number of pixels in images.

$$\text{Global accuracy} = \frac{TP+TN}{TP+FP+FN+TN} \quad (2)$$

where the false positive is denoted as FP, and the false negative is denoted as FN.

Accuracy is a metric show the percentage of the correctly classified pixels in each class compared to the total number of pixels in that class. It is given as:

$$\text{Accuracy score} = \frac{TP}{TP+FN} \quad (3)$$

Mean accuracy is an expression of the average accuracy of all classes in images.

3.1.2. Jaccard index IoU

IoU is a measure of the overlap between the ground truth in the dataset and the resulting image was generated by our model. This metric is calculated by dividing the area of the overlap between the ground truth image and the resulting image by the area of a union. The union is an area which is combined with the ground truth and the resulting image. The threshold value of *IoU* larger or equal 0.5 to decide the segmentation result is good. If *IoU* equal 1, the overlap between X and Y is perfect.

IoU is calculated by dividing the size of the intersection between the predicted image, which is generated by SegNet architecture, and the actual ground truth by the size of the union of the predicted image and the ground truth image. An *IoU* threshold of 0.5 is defined as the value. The segmentation result is supposed to be good if the *IoU* is larger than or equal to 0.5, or *IoU* threshold. If *IoU* equal 1, the overlap between the predicted set of pixels X and the ground truth Y is perfect. *IoU* can be calculated using (4):

$$IoU = J(X, Y) = \frac{|X \cap Y|}{|X| + |Y| - |X \cap Y|} \quad (4)$$

$$0 \leq IoU \leq 1$$

Mean *IoU* is the average *IoU* score of all classes in all images.

Weighted *IoU* is the average *IoU* of each class. It is weighted by the number of pixels in that class. Weighted *IoU* is used to reduce the impact of errors in small classes because images have classes with disproportionate size.

3.1.3. The boundary F1 (BF) contour matching score

The boundary F1 (BF) contour matching score ($F_1 - score$) is a novel semantic contour-based score [15]. This metric indicates how well the predicted boundary of each class aligns with the true boundary. The F-score is calculated using the precision p and the recall r , where p is calculated by dividing the number of correct classification by the all actual positive result

$$p = \frac{TP}{TP + FP} \quad (5)$$

Recall r is the number of true positive results divided by the sum of TP and FN.

$$r = \frac{TP}{TP + FN} \quad (6)$$

Finally, the $F_1 - score$ is defined as:

$$F_1 - score = \frac{2 \cdot p \cdot r}{p + r} \quad (7)$$

The $F_1 - score$ range is from 0 to 1. If the precision p and the recall r reach the perfect values, $F_1 - score$ will reach the best value.

3.2. Experiment results on dataset 1

3.2.1. Segmentation results

The size of images in dataset 1 is reduced to [360x480x3] to decrease the computation time and memory usage. Of the dataset 1, 70% (29 images and 29 corresponding ground truth images) are used for the training process, and 30% (13 images and 13 corresponding ground truth images) are used for the testing process. Two data augmentation methods, which including random reflection and random translation, are applied to training images to enlarge the number of images from 29 images to 145 images.

In our training dataset, it is observed that RBCs and background pixels occupy more areas than WBCs. This class imbalance can affect the learning process of SegNet. To solve this, class weights are used to balance the classes [14]. Class weight (w) for each class is defined as follows:

$$w = \frac{1}{f} \quad (8)$$

$$f = \frac{n}{N} \quad (9)$$

where f is the frequency of each class, n is the number of pixel in the class, and N is the total number of pixel in the image.

The last layer of SegNet architecture is updated with class weights. Class weights for three classes are shown in Table 1.

Table 2 presents the metrics to evaluate the performance of SegNet on the testing dataset. The average accuracy for the segmentation of three classes reaches 91%. The mean IoU of our model is 79%. These results have shown that a good segmentation of RBCs, WBCs, and background is obtained using our proposed method. Classification accuracy, the intersection over union (IoU), and the boundary F1 contour matching score are listed in Table 3. The true positives for white blood cells, red blood cells, and background class correspond with 94.93%, 91.11%, and 87.32% as shown in Figure 8. Figure 9 illustrates an example of WBCs and RBCs segmentation. The final result of SegNet is separate images. One of these includes all red blood cells, and the other contains a white blood cell.

Table 1. The class weights of the classes.

Name	Class weight
White Blood Cells	7.2023
Red Blood Cells	1
Background	0.6579

Table 2. Evaluation metrics of SegNet.

Global accuracy	Mean accuracy	Mean IoU	Weighted IoU	Mean BF Score
0.89	0.91	0.79	0.81	0.77

Table 3. Class metrics for three classes in images.

	Accuracy	IoU	Mean BF Score
White Blood Cells	0.95	0.75	0.62
Red Blood Cells	0.91	0.80	0.84
Background	0.87	0.82	0.84

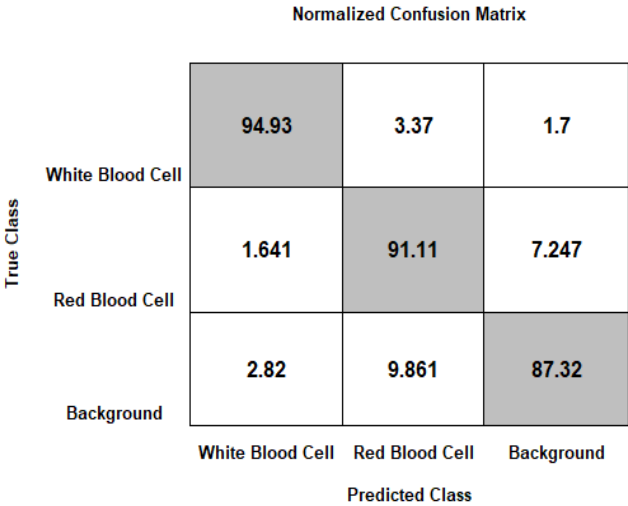


Figure 8. The confusion matrix on the testing dataset.

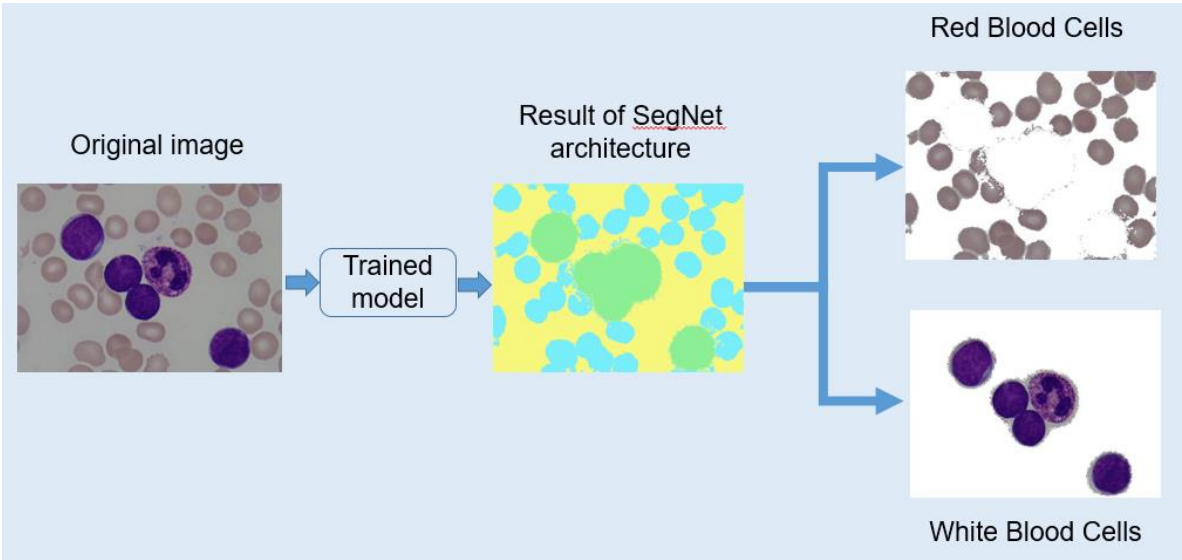


Figure 9. An example of WBCs and RBCs segmentation.

3.2.2. Results of the counting phase

In the counting phase, our method was tested on 13 images which contained only red blood cells and 13 images which contained only white blood cells. These images are the result of the segmentation phase in the previous section. Table 4 and Table 5 show the number of cells which is predicted by our method (P) and the number of actual cells in images (A).




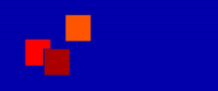
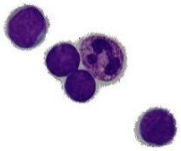
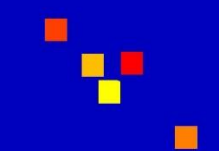


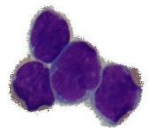
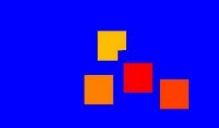

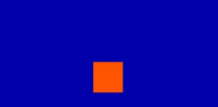

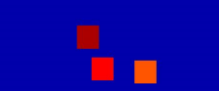


Many previous works have failed to predict the number of cells with a high degree of overlap and irregular cell shapes. On the contrary, our method can handle with high overlapping cells such as clumps of WBCs with different sizes and shapes. As shown in Table 4, the number of cells is approximately the same as that of the actual cells. Similarly, the same conclusion can be obtained with WBCs, as figured out in Table 4. Especially, with more touching WBCs composed of a clumped cell as illustrated at the first and second row of Table 4, the predicted number of WBCs are exactly the same as that of the actual cells. The accuracy of the counting phase is calculated as follows:

$$accuracy = \left(1 - \frac{|P - A|}{A}\right) \times 100 \quad (7)$$

Apparently the accuracy of all 13 WBCs images reaches 100%, as figured out in Table 4. For RBCs, Figure 10 shows that the accuracy is in the range of 81.82% to 100%. The overall accuracy of RBC count reaches 93.30%, as shown in Table 6.

Figure 11 explains the relationship of a linear regression between the numbers of RBCs, which is predicted by our method versus the numbers of actual red blood cells in images. The linear regression model of our method is represented as $y = 3.49 + 0.96x$. The coefficient of determination R^2 value is 0.89 proving that our model is able to predict the correct number of RBCs.

Table 4. The predicted (P) and actual count (A) of WBCs.

WBCs images	Segmentation of clumped cells	P	A	WBCs images	Segmentation of clumped cells	P	A
		7	7			3	3
		5	5			2	2
		4	4			1	1
		3	3			1	1

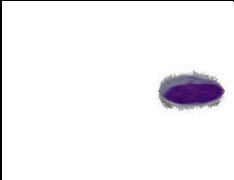
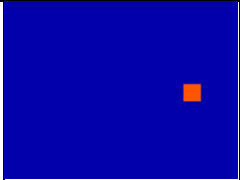
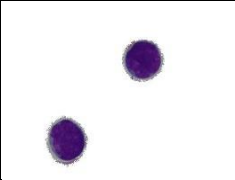
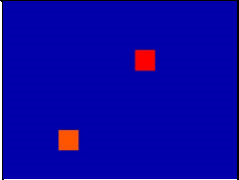
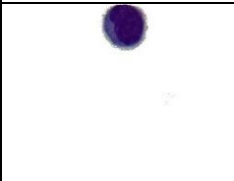
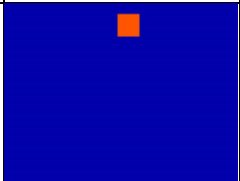
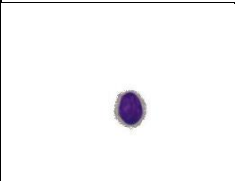
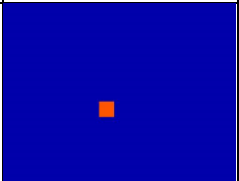
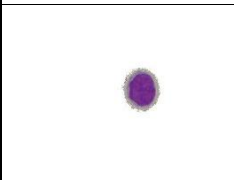
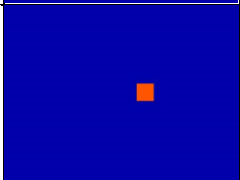
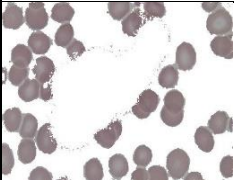
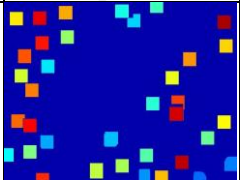
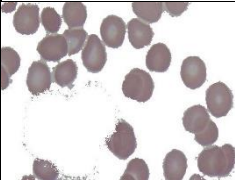
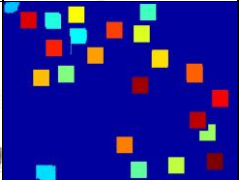


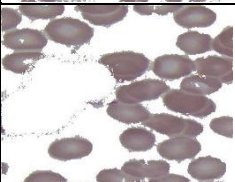
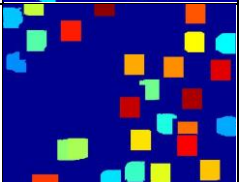


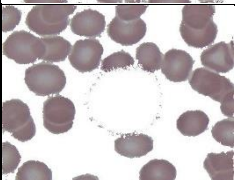
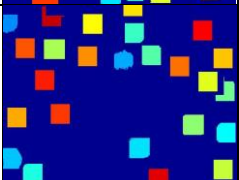
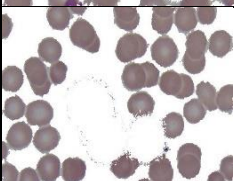
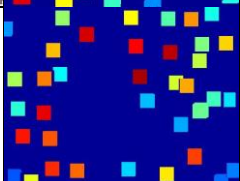
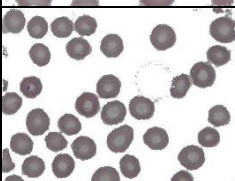
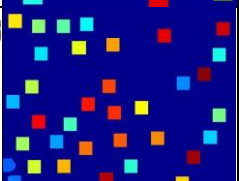


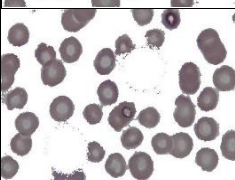
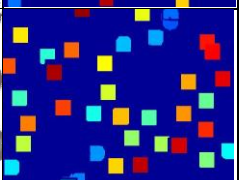
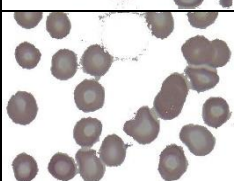
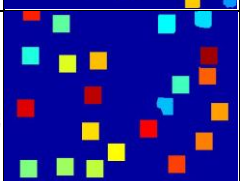
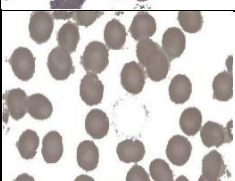
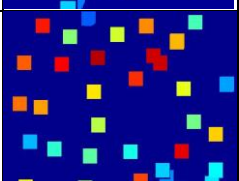
		1	1			2	2
		1	1			1	1
		1	1				

Table 5. The predicted (P) and actual count (A) of RBCs.

RBCs images	Segmentation of clumped cells	P	A	RBCs images	Segmentation of clumped cells	P	A
		36	40			23	24
		31	31			27	33
		26	30			25	30
		37	44			35	35
		30	29			38	38
		22	23			33	33

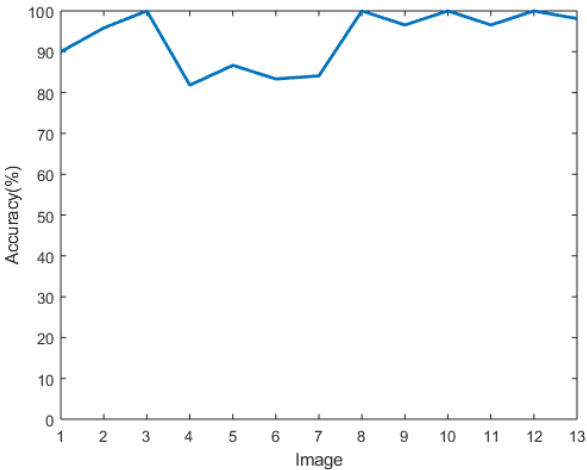
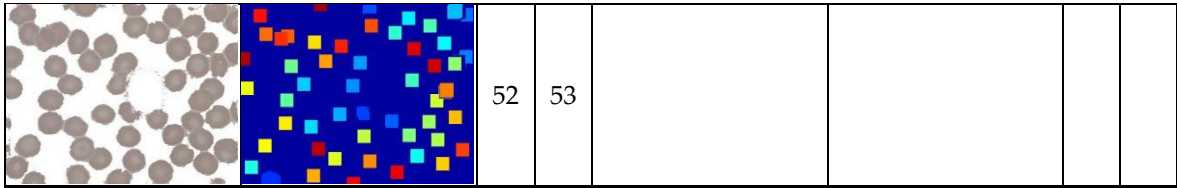


Figure 10. The accuracy for 13 red blood cell images.

Table 6. The accuracy of RBC count.

Image	Predicted number	Actual number	Accuracy (%)
1	36	40	90
2	23	24	95.83
3	31	31	100
4	27	33	81.82
5	26	30	86.67
6	25	30	83.33
7	37	44	84.09
8	35	35	100
9	30	29	96.55
10	38	38	100
11	22	23	96.55
12	33	33	100
13	52	53	98.11
			Overall accuracy: 93.30

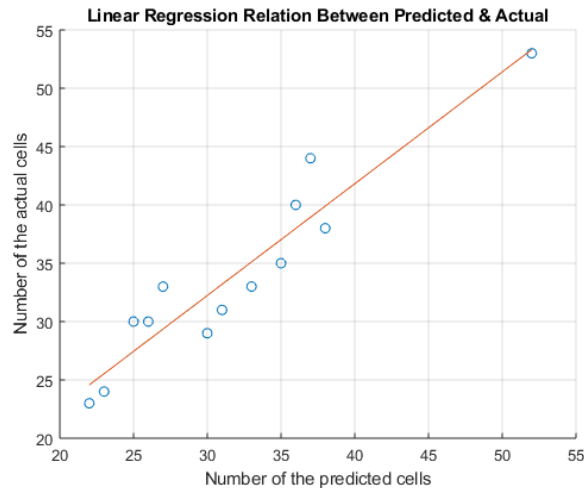


Figure 11. The linear regression relation between the number of predicted red blood cells and the number of actual red blood cells.

3.3. Experiment results on dataset 2

3.3.1. Segmentation results

Each image in dataset 1 contains only a few white blood cells. Hence, dataset 2 with more white blood cells in each image is used to evaluate our proposed system. In this paper, we use the original ALL-IDB1 image database which consists of 49 acute lymphoblastic leukemia (ALL) images and 59 peripheral blood cells images from non-leukemia people. 108 corresponding labeled images are also used as the ground truth for training and testing. The size of images in the dataset 2 is [360x480x3], same as the image size of dataset 1. 70% images in dataset 2 (76 original images and 76 corresponding ground truth images) are used for training phase. Data augmentation is also applied to the training dataset to increase the number of training images to 380 images. Similar to the segmentation on dataset 1, 30% of original images (32 images) are used for testing phase.

This section focuses on the segmentation of white blood cells from the rest cells in the image. Therefore all red blood cells and background of images are labeled as yellow, and white blood cells are annotated as green, as illustrated in Figure 12. The global accuracy and the mean accuracy of this model on dataset 2 both reach 98%. By applying formula (4), the mean IoU and weighted IoU reach 78.82% and 97.3%, respectively. The mean BF score is 89.14%. All segmentation metrics obtained from dataset 2 are higher than those obtained from dataset 1. Table 8 shows the result of dataset 2.

Class metrics for each class of dataset 2 is shown in Table 9. The accuracy and the Mean BF Score of white blood cells class in dataset 2 are higher than those of dataset 1, 97.72% and 86.13% respectively. However, the IoU of white blood cells classification in dataset 2 is lower than in dataset 1, 59.14% and 75.04% respectively.

True positives for white blood cells class of dataset 2 is 97.72%, as shown in Figure 13.

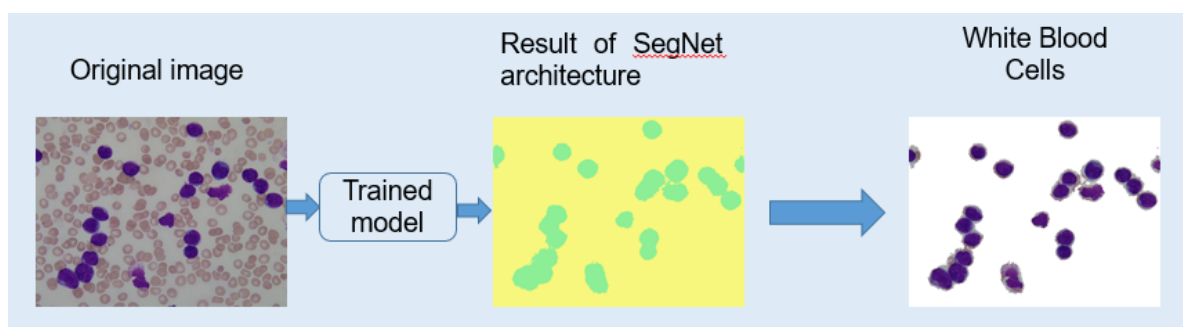


Figure 12. An example of white blood cell classification in dataset 2.

Table 7. The class weights of the classes.

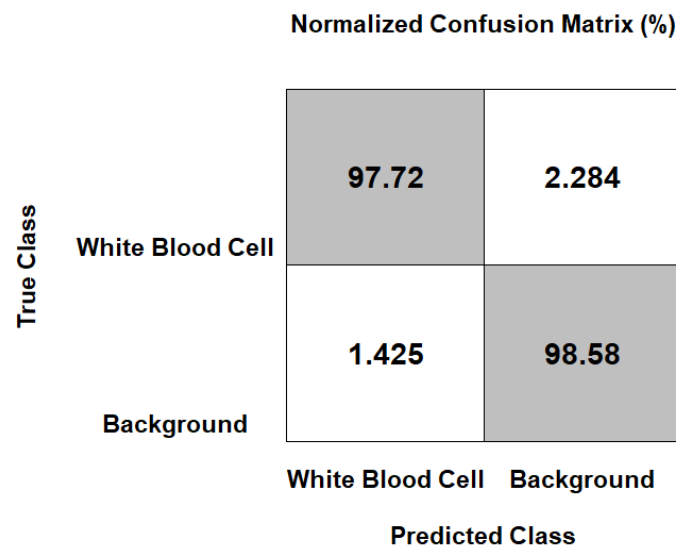
Name	Class weight
White Blood Cells	18.4013
Red Blood Cells and background	0.5140

Table 8. Semantic segmentation metrics of the model on the dataset 2.

Global accuracy	Mean accuracy	Mean IoU	Weighted IoU	Mean BF Score
0.98549	0.98145	0.78816	0.97298	0.91308

Table 9. The class metrics for white blood cells class and background class.

	Accuracy	IoU	Mean BF Score
White Blood Cells	0.97716	0.59136	0.86127
Background	0.98575	0.98495	0.9541

**Figure 13.** The confusion matrix for the testing phase of the dataset 2.

3.3.2. Results of the counting phase

We selected 12 images with the highest overlap of WBCs to be shown in Table 9. The predicted number and the actual number of 32 white blood cells images are shown in Table 10. For images with less WBCs, the accuracy of WBC count can reach up to 100%. For images with more WBCs and high overlapping WBCs, the accuracy fluctuates between 75% and 100%, as can be seen in Figure 15.

As shown in Figure 14, a linear regression between the predicted white blood cells and the actual white blood cells in images is represented as $y = -0.0071 + 1.071x$. The coefficient of determination R^2 value is 0.99. R^2 value proves that our model can predict the data very well.

Table 10. The predicted (P) and the actual count (A) of white blood cells in some images which have clumped white blood cells.

WBCs images	Segmentation of clumped cells	P	A	WBCs images	Segmentation of clumped cells	P	A
-------------	-------------------------------	---	---	-------------	-------------------------------	---	---

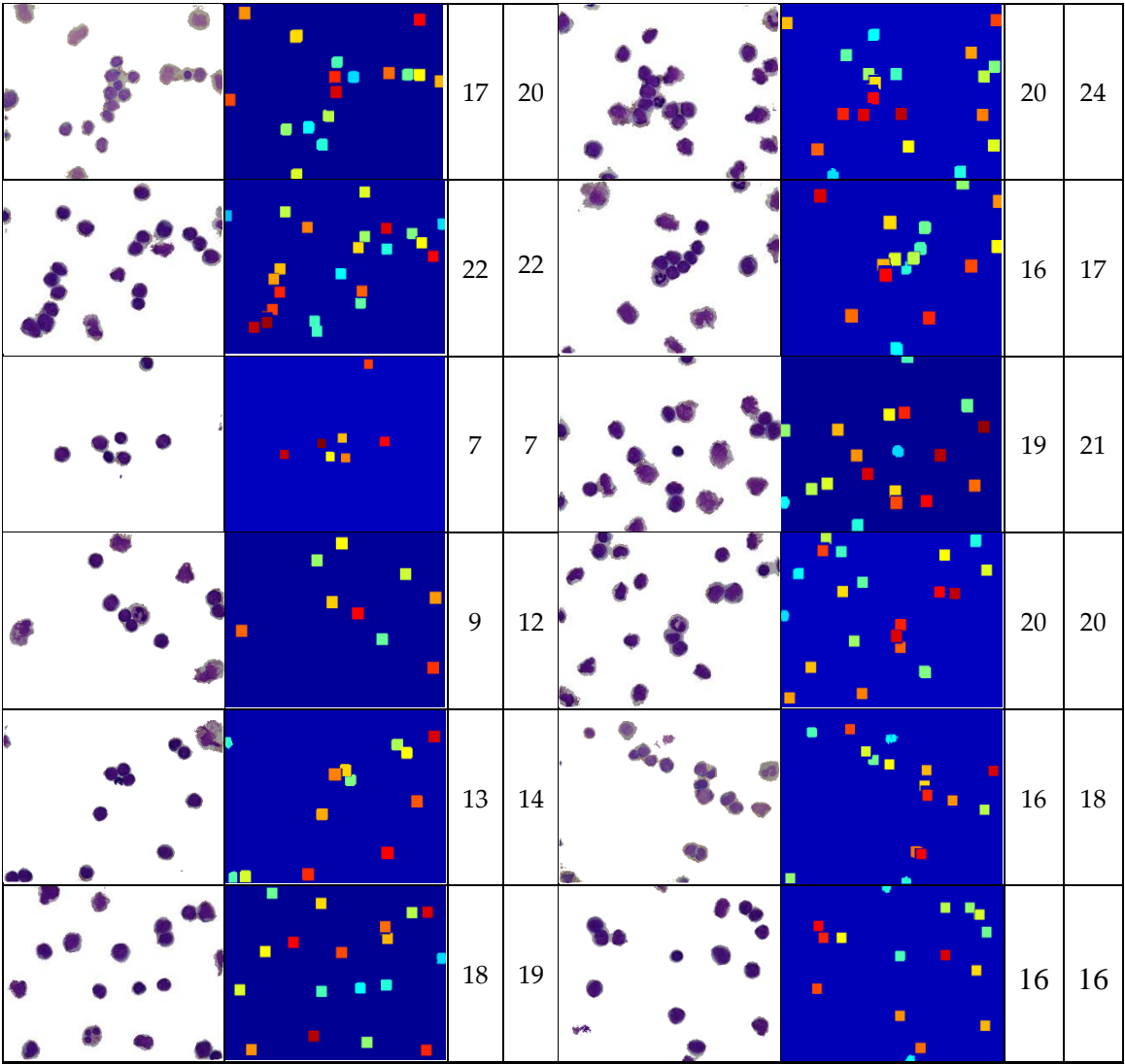


Table 11. The accuracy of WBC count.

No of mage	Predicted number	Actual number	Accuracy (%)
1	4	4	100
2	17	20	85
3	1	1	100
4	6	6	100
5	2	2	100
6	1	1	100
7	20	23	86.96
8	1	1	100
9	2	2	100
10	22	22	100
11	1	1	100
12	16	17	94.12
13	2	2	100
14	2	2	100
15	1	1	100
16	7	7	100
17	2	2	100

18	19	21	90.48
19	9	12	75
20	20	20	100
21	2	2	100
22	1	1	100
23	4	4	100
24	2	2	100
25	1	1	100
26	13	14	92.86
27	12	12	100
28	1	1	100
29	2	2	100
30	16	18	88.89
31	18	18	100
32	16	16	100
			Overall
			accuracy: 97.29

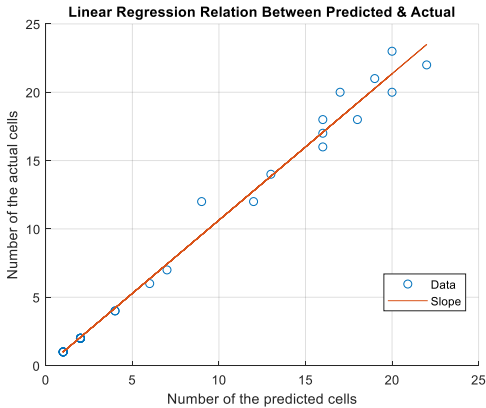


Figure 14. Linear regression relation between the number of predicted white blood cells and the number of actual white blood cells.

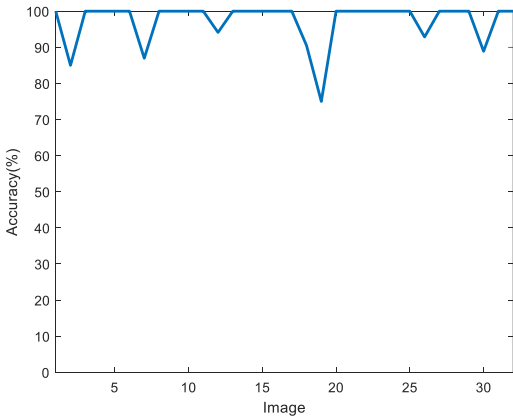


Figure 15. The accuracy for 32 WBCs images.

3.4. Comparison with current works

Our method is compared with other previous work in literature. Most researches in the past focused only on classifying and counting RBCs or WBCs. In this paper, we not only classify RBCs and WBCs simultaneously but also count both RBCs and WBCs. It is noted that our method obtains

accuracy far greater than those using other methods such as Neural Network, Bayesian model, or Circular Hough Transform for RBC count, as shown in Table 11.

In addition, most previous works utilized watershed segmentation for the segmentation of WBCs which are connected or overlapped in order to count the number of WBCs. By applying deep learning in segmentation, we can achieve an accuracy which outperforms that achieved by using state-of-the-art techniques, as presented in Table 12. In [11], Lorenzo Putzu et. al. evaluated their method in the ALL-IDB1 dataset, same dataset with our research. The ALL-IDB1 dataset contains the diversity of images. These images are acquired by different camera and different light condition. For testing purpose, Lorenzo Putzu et. al. used 33 images of ALL-IDB1 which acquired from the same lighting condition and same camera. Their method obtained the accuracy of 92%. On the contrary, our method is tested on the 32 images which is random chosen from ALL-IDB1. Our method reaches 97.29% for WBC count, significantly higher than Lorenzo Putzu's method.

Table 12. Comparison of red blood cell count with other methods.

Method	Average Accuracy (%)
Neural Network [4] (2008)	74
Bayesian model [6] (2009)	82.5
Neural network [5] (2011)	81
Circular Hough Transform [7] (2014)	91.87
Proposed method	93.3

Table 13. Comparison of white blood cell count with other methods.

Method	Average Accuracy (%)
Image processing and mathematical morphology methods [10] (2014)	85
Image processing techniques, Agglomerate identification through roundness analysis, distance transform, watershed segmentation, watershed line refining [11] (2014)	92
Color space conversion models, watershed conversion [11] (2016)	93
Proposed method	97.38

4. Conclusions

The aim of this paper is to segment WBCs and RBCs in the peripheral blood cell images into distinguishing images. A follow-on step has built on these earlier images and also strengthened the clumped cell segmentation, as well as blood cells count. WBC and RBC segmentation plays a critical role in helping doctors early diagnose some sign of the diseases which affected blood cells.

In this paper, SegNet - an innovative CNN architecture - are performed for the identification and segmentation of WBCs and RBCs in images. The lack of annotated images is a particular challenge for semantic segmentation. To solve this challenge, we manually label images to create standard annotation images. Due to the limited images in the dataset, data augmentation methods are performed in order to increase the number of images. From the experiments on two datasets, we conclude that SegNet is highly appropriate for segmenting WBCs and RBCs in blood images.

For the counting phase, we also have to face with a severe challenge – blood cells usually display in images as clumped or overlapped cells – and it put at risk the incorrect counting for WBCs and RBCs. In carrying out this challenge, Euclidean distance transform and binary dilation are applied on images. After segmenting clumped cells, eight neighbors connected component labeling are utilized to determine the number of cells. For the counting phase, our proposed method reaches 93.3% for RBC count in dataset 1 and 97.29% for WBC count in dataset 2.

Based on an experiment on dataset 1, we conclude that our methods proposed in the counting phase can handle accurately with clumped white blood cells. On the contrary, based on the

experiment on dataset 2, the accuracy of the counting phase decrease when handled with the image contained both single white blood cells and clumped white blood cells. Consequently, in the future work, we would like to separate single cells and clumped cells into distinct images before counting to improve the accuracy of blood cell count.

Author Contributions: Conceptualization, Thanh Tran Thi Phuong; Data curation, Thanh Tran Thi Phuong; Formal analysis, Thanh Tran Thi Phuong; Investigation, Thanh Tran Thi Phuong; Methodology, Thanh Tran Thi Phuong; Resources, Thanh Tran Thi Phuong; Software, Thanh Tran Thi Phuong; Supervision, Suk-Hwan Lee and Ki-Ryong Kwon; Validation, Ki-Ryong Kwon; Writing – original draft, Thanh Tran Thi Phuong; Writing – review & editing, Thanh Tran Thi Phuong and Lam Binh Minh.

Acknowledgments: This research was supported by Basic Science Research Program through the National Research Foundation of Korea (NRF) funded by the Ministry of Science and ICT (No. 2016R1D1A3B03931003, No. 2017R1A2B 2012456).

Conflicts of Interest: The authors declare no conflict of interest.

References

1. Complete Blood Count (CBC): Types, Preparation & Procedure. Available online: <https://www.healthline.com/health/cbc> (accessed on 13th November 2018).
2. Gao, W., Tang, Y. & Li, X. Segmentation of microscopic images for counting leukocytes. 2nd Int. Conf. Bioinforma. Biomed. Eng. iCBBE 2008, pp. 2609–2612, doi:10.1109/ICBBE.2008.985.
3. Harun, N. H., Nasir, A. S. A., Mashor, M. Y. & Hassan, R. Unsupervised Segmentation Technique for Acute Leukemia Cells Using Clustering Algorithms. *International Journal of Computer and Information Engineering* **2015**, 9, pp. 253–259.
4. Poomcokrak, J. & Neatpisarnvanit, C. Red blood cells extraction and counting. *The 3rd International Symposium on Biomedical Engineering* **2008**, pp. 199–203, doi:10.1109/ICIP.2001.959235
5. Jambhekar, N. D. Red Blood Cells Classification using Image Processing. *Science Research Reporter* **2011**, 1, pp. 151–154.
6. Vromen, J. & McCane, B. Red blood cell segmentation from SEM images. 2009 24th Int. Conf. Image Vis. Comput. New Zealand, IVCNZ 2009 - Conf. Proc. 44–49 (2009), doi:10.1109/IVCNZ.2009.5378364
7. Mazalan, S. M., Mahmood, N. H. & Razak, M. A. A. Automated red blood cells counting in peripheral blood smear image using circular hough transform. Proceedings - 1st International Conference on Artificial Intelligence, Modelling and Simulation, AIMS 2013, 1, pp. 320–324, doi:10.1109/AIMS.2013.59
8. Ruberto, C. Di, Putzu, L. White Blood Cells Identification and Counting from Microscopic Blood Image White Blood Cells Identification and Counting from Microscopic Blood Image. *International Journal of Medical, Health, Biomedical and Pharmaceutical Engineering* **2013**, 7, pp. 15–22.
9. Putzu, L., Caocci, G. and Di, C. Leucocyte classification for leukaemia detection using image processing techniques. *Artificial Intelligence In Medicine* **2014**, 62, pp. 179–191, doi:10.1016/j.artmed.2014.09.002
10. Jha, K. K., Das, B. K. & Dutta, H. S. Detection of abnormal blood cells on the basis of nucleus shape and counting of WBC. Proceeding of the IEEE International Conference on Green Computing, Communication and Electrical Engineering, ICGCCEE 2014. doi:10.1109/ICGCCEE.2014.6922219
11. Alreza, Z. K. K. & Karimian, A. Design a new algorithm to count white blood cells for classification leukemic blood image using machine vision system. 2016 6th International Conference on Computer and Knowledge Engineering, ICCKE 2016. doi:10.1109/ICCKE.2016.7802148
12. Badrinarayanan, V., Kendall, A., Cipolla, R. & Member, S. SegNet: A Deep Convolutional Encoder-Decoder Architecture for Image Segmentation. *IEEE Transactions on Pattern Analysis and Machine Intelligence* **2017**, 39, pp. 2481–2495, doi:10.1109/TPAMI.2016.2644615
13. Csurka, G., Larlus, D. & Perronnin, F. What is a good evaluation measure for semantic segmentation? Proceedings of the British Machine Vision Conference 2013. doi:10.5244/C.27.32
14. Buda, M. & Maki, A. A systematic study of the class imbalance problem in convolutional neural networks. *Neural Networks* **2018**, 106, pp. 249–259, doi:10.1016/j.neunet.2018.07.011